

# Isotropic and Anisotropic Magnetic Exchange Interactions through $\mu$ - $N^1, N^2$ 1,2,4-Triazole and $\mu$ -Sulfato Bridges: X-ray Crystal Structure, Magnetic Properties, and Single-Crystal EPR Study of $(\mu$ -4-Amino-3,5-bis(pyridin-2-yl)-1,2,4-triazole- $N^1, N^2, N''$ )( $\mu$ -sulfato- $O, O'$ )[(sulfato- $O$ )aquacopper(II)]triacuacopper(II) Hydrate

Petra J. van Koningsbruggen,<sup>1a</sup> Dante Gatteschi,<sup>1b</sup> Rudolf A. G. de Graaff,<sup>1a</sup>  
Jaap G. Haasnoot,<sup>\*1a</sup> Jan Reedijk,<sup>1a</sup> and Claudia Zanchini<sup>1c</sup>

Leiden Institute of Chemistry, Gorlaeus Laboratories, Leiden University, P.O. Box 9502,  
2300 RA Leiden, The Netherlands, Department of Chemistry, University of Florence,  
Via Maragliano 75/77, 50144 Firenze, Italy, and Department of Chemistry, University of Calabria,  
87030 Arcavacata di Rende (Cosenza), Italy

Received January 18, 1995<sup>®</sup>

The crystal and molecular structure of  $(\mu$ -4-amino-3,5-bis(pyridin-2-yl)-1,2,4-triazole- $N^1, N^2, N''$ )( $\mu$ -sulfato- $O, O'$ )-[(sulfato- $O$ )aquacopper(II)]triacuacopper(II) hydrate,  $[\text{Cu}_2(\text{abpt})(\text{SO}_4)_2(\text{H}_2\text{O})_4]\cdot\text{H}_2\text{O}$  (**1**) ( $\text{C}_{12}\text{H}_{20}\text{Cu}_2\text{N}_6\text{O}_{13}\text{S}_2$ ), in which abpt = 4-amino-3,5-bis(pyridin-2-yl)-1,2,4-triazole, was determined by X-ray diffraction methods. Crystal data for **1**:  $T = 298$  K, monoclinic, space group =  $P2_1$ , with  $a = 9.9704(3)$  Å,  $b = 14.7093(3)$  Å,  $c = 7.4034(6)$  Å,  $\beta = 96.8641(6)^\circ$ ,  $Z = 2$  (dinuclear molecules),  $V = 1078$  Å<sup>3</sup>. The least-squares refinement based on 2717 significant reflections [ $I > 2\sigma(I)$ ] converged to  $R = 0.0410$  and  $R_w = 0.0500$ . The structure of **1** consists of asymmetric dinuclear units, in which the copper(II) ions are linked in the equatorial plane by an  $N^1, N^2$  bridging chelating abpt ligand and a didentate bridging sulfate anion. The Cu–O(sulfate) distances are very short (1.937(4) and 1.908(5) Å). The Cu(1)–Cu(2) distance is 4.415(1) Å. The compound represents the first example of a dinuclear copper(II) compound having a single  $N^1, N^2$  1,2,4-triazole bridge. Both Cu(II) ions have four short equatorial distances to the bridging sulfate, the bridging 1,2,4-triazole, the pyridyl group, and a monodentate sulfate (Cu(1)) or a water molecule (Cu(2)). Cu(1) has one additional apical water molecule, whereas Cu(2) has two additional axial water molecules. Hydrogen bonding appears to play an important role in the stabilization of the asymmetric dinuclear cluster. The magnetic susceptibility data (295–6 K) are interpreted on the basis of the spin Hamiltonian  $\hat{H} = -2J[\hat{S}_{\text{Cu}(1)}\hat{S}_{\text{Cu}(2)}]$ , yielding  $J = -34.5$  cm<sup>-1</sup>,  $g = 2.15$ , and  $p = 0.66\%$ . The isotropic exchange constant is compared to the ones of doubly  $N^1, N^2$  1,2,4-triazole bridged dinuclear copper(II) compounds. The single-crystal X-band EPR spectra recorded at room temperature are typical of a triplet spin state with  $g_{xx} = 2.09(3)$ ,  $g_{yy} = 2.10(3)$ ,  $g_{zz} = 2.32(2)$ ,  $D_{xx} = 0.018(2)$  cm<sup>-1</sup>,  $D_{yy} = 0.04(3)$  cm<sup>-1</sup>, and  $D_{zz} = -0.058(3)$  cm<sup>-1</sup>. The  $g$  directions in the  $xy$  plane are affected by a large experimental error, due to the very small anisotropy of  $g$  in this plane. The  $g_{zz}$  and  $D_{zz}$  directions are almost parallel; the angle between these vectors is only  $2^\circ$ . These vectors make an angle of about  $12^\circ$  with the normal vector to the Cu(1)–Cu(2) coordination plane. The zero-field-splitting parameter  $D$  shows evidence of dominant exchange contributions, since its largest component is observed orthogonal to the Cu(1)–Cu(2) coordination plane. The magnetic and EPR data are discussed in comparison with those obtained for the doubly  $N^1, N^2$  1,2,4-triazole bridged dinuclear copper(II) derivatives.

## Introduction

The magnetic properties of copper(II) ions incorporated in various coordination compounds have been the subject of intensive study over the past few years.<sup>2–13</sup> A main reason for this interest is probably that the phenomenon of interaction between metal centers lies at the intersection of, on first sight,

widely separated areas, namely the physics of the magnetic materials and the role of polynuclear reaction sites in biological<sup>14–18</sup> and catalytic processes.<sup>19–24</sup> To maintain copper(II) ions on certain distances, bridging ligands have been found to be quite useful. Bridging systems based on the 1,2,4-triazole ring are very interesting because of their similarity to 1,3-

\* Author to whom correspondence should be addressed.

<sup>®</sup> Abstract published in *Advance ACS Abstracts*, September 1, 1995.

- (1) (a) Leiden University. (b) University of Florence. (c) University of Calabria.
- (2) Kahn, O. In *Magneto-structural correlations in exchange coupled systems*; Gatteschi, D., Kahn, O., Willett, R. D., Eds.; NATO Advanced Study Institute Series; D. Reidel: Dordrecht, Holland, 1984; Vol. C140.
- (3) Cairns, C. J.; Busch, D. H. *Coord. Chem. Rev.* **1986**, *69*, 1.
- (4) Kahn, O. *Angew. Chem., Int. Ed. Engl.* **1985**, *24*, 834.
- (5) Bencini, A.; Gatteschi, D.; Zanchini, C.; Haasnoot, J. G.; Prins, R.; Reedijk, J. *J. Am. Chem. Soc.* **1987**, *109*, 2926.
- (6) Prins, R.; de Graaff, R. A. G.; Haasnoot, J. G.; Vader, C.; Reedijk, J. *J. Chem. Soc., Chem. Commun.* **1986**, 1430.
- (7) Bencini, A.; Gatteschi, D.; Zanchini, C.; Haasnoot, J. G.; Prins, R.; Reedijk, J. *Inorg. Chem.* **1985**, *24*, 2812.

- (8) Prins, R.; Birker, P. J. M. W. L.; Haasnoot, J. G.; Verschoor, G. C.; Reedijk, J. *Inorg. Chem.* **1985**, *24*, 4128.
- (9) Koomen-van Oudenniel, W. M. E.; de Graaff, R. A. G.; Haasnoot, J. G.; Prins, R.; Reedijk, J. *Inorg. Chem.* **1989**, *28*, 1128.
- (10) van Koningsbruggen, P. J.; Haasnoot, J. G.; de Graaff, R. A. G.; Reedijk, J.; Slingerland, S. *Acta Crystallogr.* **1992**, *C48*, 1923.
- (11) Slangen, P. M.; van Koningsbruggen, P. J.; Haasnoot, J. G.; Jansen, J.; Gorter, S.; Reedijk, J.; Kooijman, H.; Smeets, W. J. J.; Spek, A. L. *Inorg. Chim. Acta* **1993**, *212*, 289.
- (12) Slangen, P. M.; van Koningsbruggen, P. J.; Goubitz, K.; Haasnoot, J. G.; Reedijk, J. *Inorg. Chem.* **1994**, *33*, 1121.
- (13) van Koningsbruggen, P. J.; van Hal, J. W.; Müller, E.; de Graaff, R. A. G.; Haasnoot, J. G.; Reedijk, J. *J. Chem. Soc., Dalton Trans.* **1993**, 1371.
- (14) Solomon, E. I. In *Copper proteins*; Spiro, T. G., Ed.; Wiley-Interscience: New York, 1981; p 2.
- (15) Vigato, P. A.; Tamburini, S. *Coord. Chem. Rev.* **1990**, *106*, 25.

imidazolate bridging found in the copper–zinc protein superoxide dismutase.<sup>16</sup> To investigate the correlation between the magnetic superexchange mechanism, structural features, and ligand coordination properties more thoroughly, a series of copper(II) compounds of related N-donating substituted 1,2,4-triazole ligands forming five-membered chelate rings has been studied.<sup>5–12</sup> By the analysis of the magnetic and structural data for various dinuclear copper(II) compounds, in which the metal ions are linked in the equatorial coordination plane by two  $N^1, N^2$  bridging 1,2,4-triazole ligands,<sup>7–12</sup> it became evident that the singlet–triplet splittings vary with the Cu–N(1)–N(2) angle (N(1) and N(2) being the bridging 1,2,4-triazole nitrogen atoms).<sup>11,12</sup> It has been shown experimentally that in case of the most symmetric  $N^1, N^2$  1,2,4-triazole bridging mode in the equatorial plane, *i.e.*, with all Cu–N–N angles close to 135° and with N–Cu–N innermost angles close to 90°, the largest possible absolute value for  $-2J$  is of the order of 240 cm<sup>-1</sup>.<sup>12</sup> A more asymmetric bridging mode will lead to a less efficient magnetic orbital overlap, and the isotropic exchange constant decreases. These results represented one of the first successful magneto–structural correlations for copper(II) ions linked *via* double diatomic bridges, between the isotropic exchange constant, characterizing the interaction between the copper(II) ground magnetic orbitals, and its structural parameters. On the other hand, for this type of dinuclear copper(II) compound, less is known about the anisotropic exchange constant, which accounts for the interaction between the ground state magnetic orbital of one copper(II) ion and the excited state magnetic orbital of the other copper(II) ion. This information can be obtained from single-crystal EPR data, where from the analysis of the axial zero-field-splitting tensor, **D**, the magnitude of its dipolar and exchange determined components can be calculated.<sup>25,26</sup> A single-crystal EPR study for [Cu(bpt)(CF<sub>3</sub>SO<sub>3</sub>)(H<sub>2</sub>O)]<sub>2</sub> (bpt = 3,5-bis(pyridin-2-yl)-1,2,4-triazolato)<sup>7</sup> has shown that exchange contributes considerably to the axial zero-field splitting. These results were in agreement with the single-crystal EPR study on [Cu(ppt)(H<sub>2</sub>O)]<sub>4</sub>(NO<sub>3</sub>)<sub>4</sub>(H<sub>2</sub>O)<sub>12</sub> (ppt = 3-(pyridin-2-yl)-5-(pyrazin-2-yl)-1,2,4-triazolato).<sup>5</sup>

In this paper, the crystal structure of the first dinuclear copper(II) compound containing a single  $N^1, N^2$  1,2,4-triazole bridge is described. The compound, [Cu<sub>2</sub>(abpt)(SO<sub>4</sub>)<sub>2</sub>(H<sub>2</sub>O)<sub>4</sub>]·H<sub>2</sub>O (**1**), is obtained by the reaction of CuSO<sub>4</sub>·5H<sub>2</sub>O with 4-amino-3,5-bis(pyridin-2-yl)-1,2,4-triazole (abbreviated as abpt). Furthermore, by a change in the abpt to copper(II) sulfate pentahydrate ratio a mononuclear cluster of composition [Cu(abpt)<sub>2</sub>(H<sub>2</sub>O)](HSO<sub>4</sub>)<sub>2</sub> has been obtained, which is described elsewhere.<sup>27</sup> Other studies dealt with dinuclear<sup>28</sup> and mononuclear<sup>29–32</sup> transition-metal compounds of abpt. The study of the magnetic

properties of [Cu<sub>2</sub>(abpt)(SO<sub>4</sub>)<sub>2</sub>(H<sub>2</sub>O)<sub>4</sub>]·H<sub>2</sub>O allows a comparison of the isotropic and anisotropic exchange constants for singly and doubly  $N^1, N^2$  1,2,4-triazole bridged dinuclear copper(II) compounds.

## Experimental Section

**Materials.** Commercially available solvents and copper(II) sulfate pentahydrate were used without further purification. The ligand abpt was synthesized according to the method of Geldard and Lions<sup>33</sup> from 2-cyanopyridine (Fluka AG) and hydrazine hydrate (Janssen Chimica) as starting materials.

**Synthesis of [Cu<sub>2</sub>(abpt)(SO<sub>4</sub>)<sub>2</sub>(H<sub>2</sub>O)<sub>4</sub>]·H<sub>2</sub>O (**1**).** A 5 mmol (1.19 g) sample of abpt dissolved in 30 mL of methanol was added to 10 mmol (2.42 g) of CuSO<sub>4</sub>·5H<sub>2</sub>O in 10 mL of hot water. The hot solution was filtered, and after a few days the light blue compound crystallized upon slow evaporation of the solvent at room temperature. Yield: 40%. Anal. Calc for C<sub>12</sub>H<sub>20</sub>Cu<sub>2</sub>N<sub>6</sub>O<sub>13</sub>S<sub>2</sub>: Cu, 19.63; C, 22.26; H, 3.11; N, 12.98. Found: Cu, 20.21; C, 22.17; H, 3.00; N, 13.01.

**Elemental Analyses.** C, H, N, and Cu determinations were performed by the Microanalytical Laboratory of University College, Dublin, Ireland.

**IR and Electronic Spectra.** Infrared spectra were recorded as KBr pellets in the range 4000–250 cm<sup>-1</sup> on a Perkin-Elmer 580B spectrophotometer. UV/visible spectra were obtained on a Perkin-Elmer 330 spectrophotometer using the diffuse-reflectance technique with MgO as a reference.

**EPR Spectra.** X-Band powder (*ca.* 9 GHz) EPR spectra (298–20 K) was obtained on a JEOL RE2x electron spin resonance spectrometer using an ESR900 continuous-flow cryostat. Q-Band (*ca.* 34.4 GHz) powder EPR at 22 K was performed on a Varian E-9 spectrometer with a Bruker ER061SR microwave bridge. EPR-suitable single crystals of **1** were oriented with a Philips PW1100 diffractometer and were found to correspond to the observed structure with well-developed (001), (010), and (100) faces. Single-crystal EPR spectra were recorded at room temperatures on a Varian E-9 spectrometer equipped with standard X-band (9.53 GHz) facilities.

**Magnetic Measurements.** Magnetic susceptibilities were measured in the temperature range 295–6 K with a fully automated Manics DSM-8 susceptometer equipped with a TBT continuous-flow cryostat and a Drusch EAF 16 NC electromagnet operating at *ca.* 1.4 T. Data were corrected for magnetization of the sample holder and for diamagnetic contributions, which were estimated from the Pascal constants. Magnetic data were fitted to theoretical expressions by means of a Simplex routine.<sup>34</sup> All parameters (*J*, *g*, and *p*, the amount of paramagnetic impurity) were varied independently during the fitting procedure. This routine minimizes the function  $R = [\sum |\chi_{\text{obs}} - \chi_{\text{calc}}|^2 / \sum \chi_{\text{obs}}^2]^{1/2}$ .

**Crystallographic Data Collection and Refinement of the Structure.** The structure of compound **1** was solved by X-ray diffraction. Parameters for data collection and refinement are given in Table 1. A clear light blue crystal, block shaped, of approximate dimensions 0.25 × 0.25 × 0.25 mm was mounted in a Lindemann capillary. X-ray data were collected at 298 K on an Enraf-Nonius CAD-4 four-circle diffractometer with graphite-monochromated Mo K $\alpha$  radiation ( $\lambda = 0.71073$  Å). Cell constants were determined from setting angles of 24 reflections ( $8^\circ < \theta < 12^\circ$ ). Intensity data were collected with  $2^\circ < \theta < 35^\circ$ , by using an  $\omega$ - $2\theta$  scan. A total of 2717 unique reflections were collected for which  $I > 2\sigma(I)$ . The intensities were corrected for Lorentz and polarization effects. Absorption correction was applied on the basis of the shape of the crystal and subsequent calculation of

(16) Feiters, M. C. *Comments Inorg. Chem.* **1990**, *11*, 131.

(17) Solomon, E. I.; Baldwin, M. J.; Lowery, M. D. *Chem. Rev.* **1992**, *92*, 521.

(18) Sorrell, T. N. *Tetrahedron* **1989**, *45*, 3.

(19) Schouten, J.; Challa, G.; Reedijk, J. *J. Mol. Catal.* **1980**, *9*, 41.

(20) Rogic, M. M.; Demmin, T. R. *J. Am. Chem. Soc.* **1978**, *100*, 5472.

(21) Endres, G. F.; Hay, A. S.; Eustace, J. W. *J. Org. Chem.* **1963**, *28*, 1300.

(22) Challa, G.; Chen, W.; Reedijk, J. *Macromol. Chem., Macromol. Symp.* **1992**, *59*, 59.

(23) Meinders, H. C.; van Bolhuis, F.; Challa, G. *J. Mol. Catal.* **1979**, *5*, 225.

(24) Reedijk, J. *Bioinorganic Catalysis*; Marcel Dekker: New York, 1993.

(25) Bencini, A.; Gatteschi, D. *EPR of Exchange Coupled Systems*; Springer-Verlag: Berlin, Heidelberg, 1990.

(26) Bencini, A.; Gatteschi, D. In *Transition Metal Chemistry*; Melson, G. A., Figgis, B. N., Eds.; Marcel Dekker: New York, 1982; Vol. 8, p 1.

(27) van Koningsbruggen, P. J.; Goubitz, K.; Haasnoot, J. G.; Reedijk, J. In preparation; to be submitted to *Inorg. Chim. Acta*.

(28) Keij, F. S.; de Graaff, R. A. G.; Haasnoot, J. G.; Reedijk, J. *J. Chem. Soc., Dalton Trans.* **1984**, 2093.

(29) Faulmann, C.; van Koningsbruggen, P. J.; de Graaff, R. A. G.; Haasnoot, J. G.; Reedijk, J. *Acta Crystallogr.* **1990**, *C46*, 2357.

(30) Garcia, M. P.; Manero, J. A.; Oro, L. A.; Apreda, M. C.; Cano, F. H.; Foces-Foces, C.; Haasnoot, J. G.; Prins, R.; Reedijk, J. *Inorg. Chim. Acta* **1986**, *122*, 235.

(31) Cornelissen, J. P.; van Diemen, J. H.; Groeneveld, L. R.; Haasnoot, J. G.; Spek, A. L.; Reedijk, J. *Inorg. Chem.* **1992**, *31*, 198.

(32) Kunkeler, P. J.; van Koningsbruggen, P. J.; Cornelissen, J. P.; van der Kraan, A. M.; Spek, A. L.; Haasnoot, J. G.; Reedijk, J. Submitted to *J. Am. Chem. Soc.*

(33) Geldard, J. F.; Lions, F. *J. Org. Chem.* **1965**, *30*, 318.

(34) Nelder, J. A.; Mead, R. *Comput. J.* **1965**, *7*, 308.

**Table 1.** Crystallographic Data and Details of the Structure Determination for  $[\text{Cu}_2(\text{abpt})(\text{SO}_4)_2(\text{H}_2\text{O})_4]\cdot\text{H}_2\text{O}$ 

chem formula	mol wt 647.53
$\text{C}_{12}\text{H}_{20}\text{Cu}_2\text{N}_6\text{O}_{13}\text{S}_2$	monoclinic, space group
$a = 9.9704(3) \text{ \AA}$	$P2_1$ (No. 4)
$b = 14.7093(3) \text{ \AA}$	cryst size $0.25 \times 0.25 \times$
$c = 7.4034(6) \text{ \AA}$	$0.25 \text{ mm}^3$
$\beta = 96.8641(6)^\circ$	$\lambda = 0.710 \text{ 73 \AA}$ (Mo K $\alpha$ )
$\rho_{\text{obs}} = 2.00(1) \text{ g cm}^{-3}$ ,	$\rho_{\text{calc}} = 2.00 \text{ g cm}^{-3}$
$V = 1078 \text{ \AA}^3$	$F(000) = 656$
$Z = 2$ (dinuclear units)	$\theta$ range $2-35^\circ$
$\mu(\text{Mo K}\alpha) = 22.22 \text{ cm}^{-1}$	$T = 290 \text{ }^\circ\text{C}$
no. of tot. data = 5180	weights $1/(\sigma^2(F) +$
no. of obsd data	$0.0025F^2)$
$[I > 2\sigma(I)] = 2717$	final $R^a = 0.0411$
no. of params = 317	final $R_w^a = 0.0500$
dataset $h, k, l: -16$ to	
$+16, 0-23, 0-11$	

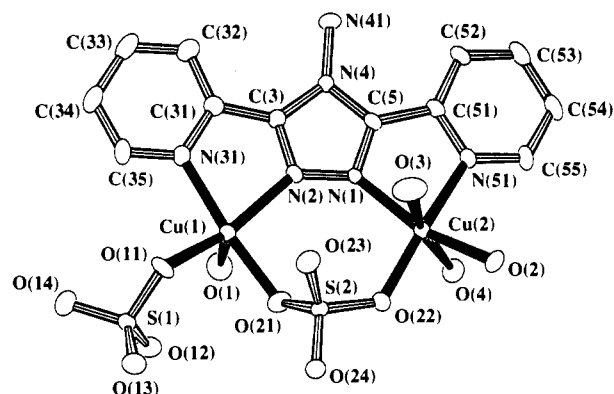
$$^a R = \sum(|F_o| - |F_c|)/\sum|F_o|, \quad ^b R_w = [\sum w(|F_o| - |F_c|)^2/\sum w|F_o|^2]^{1/2}.$$

**Table 2.** Final Coordinates ( $\times 10^4$ ) and Equivalent Isotropic Thermal Parameters ( $\times 10^3$  for Cu and S;  $\times 10^2$  for All Other Atoms) of the Non-Hydrogen Atoms of  $[\text{Cu}_2(\text{abpt})(\text{SO}_4)_2(\text{H}_2\text{O})_4]\cdot\text{H}_2\text{O}^a$ 

atom	$x/a$	$y/b$	$z/c$	$B(\text{iso}),^b \text{ \AA}^2$
Cu(1)	1366(1)	-919(4)	-1976(1)	1658(15)
Cu(2)	3368(1)	1442(4)	875(1)	1810(20)
S(1)	1793(2)	-3003(4)	-2063(3)	1610(30)
O(11)	1075(6)	-2164(5)	-1525(8)	244(12)
O(12)	2868(5)	-2713(5)	-3146(7)	233(12)
O(13)	2352(5)	-3466(5)	-402(7)	279(13)
O(14)	818(5)	-3549(6)	-3204(8)	317(13)
S(2)	3470(2)	-660(4)	1196(3)	1640(30)
O(21)	3197(5)	-883(6)	-761(5)	241(11)
O(22)	4134(5)	262(5)	1321(8)	228(12)
O(23)	2184(5)	-589(5)	1950(7)	240(11)
O(24)	4397(5)	-1312(5)	2134(8)	258(12)
N(1)	1767(5)	1191(5)	-1039(8)	163(12)
N(2)	1048(6)	456(6)	-1771(9)	198(13)
C(3)	-126(6)	736(6)	-2576(9)	157(13)
N(4)	-195(5)	1660(5)	-2388(8)	153(11)
C(5)	991(6)	1905(6)	-1420(9)	160(13)
C(31)	-1060(7)	65(6)	-3477(9)	179(14)
N(31)	-543(5)	-785(5)	-3315(8)	185(12)
C(32)	-2340(8)	245(7)	-4327(11)	250(20)
C(33)	-3084(7)	-500(7)	-5071(11)	270(20)
C(34)	-2548(8)	-1379(7)	-4889(11)	280(20)
C(35)	-1291(7)	-1487(7)	-4021(11)	240(20)
C(51)	1500(6)	2802(6)	-859(9)	172(13)
N(51)	2693(5)	2736(5)	196(8)	177(12)
C(52)	897(7)	3628(5)	-1368(11)	197(15)
C(53)	1598(8)	4418(6)	-856(11)	250(20)
C(54)	2874(8)	4346(6)	138(11)	240(20)
C(55)	3377(8)	3502(7)	658(12)	250(20)
N(41)	-1253(6)	2256(5)	-2967(8)	229(13)
O(1)	2521(5)	-911(6)	-4401(7)	284(12)
O(2)	4527(5)	1920(5)	3061(7)	225(11)
O(3)	1839(6)	1246(7)	3132(11)	440(20)
O(4)	5088(5)	1869(5)	-1031(8)	258(12)
O(5)	-4410(8)	-4241(7)	4032(9)	480(20)

<sup>a</sup> Estimated standard deviations are given in parentheses. <sup>b</sup>  $B(\text{iso}) = (8/3)\pi^2 \text{ trace}(U)$ .

the transmission integral by Monte-Carlo methods.<sup>35</sup> The copper atom was located from a Patterson map. The structure was solved by automatic Fourier techniques, using the computer program AUTO-FOUR.<sup>36</sup> The refinement of the structure with a local least-squares program led to a final  $R$  value of 0.0410 ( $R_w = 0.0500$ ), including 2717 observations and 317 parameters. Least-squares techniques were used for the refinement of non-hydrogen atom positional and anisotropic thermal parameters. Hydrogen atoms belonging to the water molecules

**Figure 1.** ORTEP<sup>38</sup> projection showing the structure and the atomic labeling of  $[\text{Cu}_2(\text{abpt})(\text{SO}_4)_2(\text{H}_2\text{O})_4]\cdot\text{H}_2\text{O}$ .**Table 3.** Bond Distances ( $\text{\AA}$ ) for  $[\text{Cu}_2(\text{abpt})(\text{SO}_4)_2(\text{H}_2\text{O})_4]\cdot\text{H}_2\text{O}^a$ 

Cu(1)—Cu(2)	4.415(1)	C(32)—C(33)	1.40(1)
Cu(1)—O(11)	1.891(5)	C(33)—C(34)	1.40(1)
Cu(1)—O(21)	1.937(4)	C(34)—C(35)	1.35(1)
Cu(1)—N(2)	2.056(6)	C(35)—N(31)	1.342(8)
Cu(1)—N(31)	2.048(5)	N(31)—C(31)	1.353(8)
Cu(1)—O(1)	2.247(5)	C(5)—C(51)	1.455(9)
Cu(2)—O(22)	1.908(5)	C(51)—C(52)	1.388(9)
Cu(2)—N(1)	2.038(5)	C(52)—C(53)	1.385(9)
Cu(2)—N(51)	2.061(6)	C(53)—C(54)	1.40(1)
Cu(2)—O(2)	2.001(5)	C(54)—C(55)	1.38(1)
Cu(2)—O(3)	2.411(7)	C(55)—N(51)	1.340(9)
Cu(2)—O(4)	2.430(5)	N(51)—C(51)	1.347(8)
N(1)—N(2)	1.372(8)	S(1)—O(11)	1.504(5)
N(2)—C(3)	1.314(8)	S(1)—O(12)	1.476(5)
C(3)—N(4)	1.370(8)	S(1)—O(13)	1.457(5)
N(4)—N(41)	1.399(7)	S(1)—O(14)	1.451(5)
N(4)—C(5)	1.356(8)	S(2)—O(21)	1.478(5)
C(5)—N(1)	1.315(8)	S(2)—O(22)	1.508(5)
C(3)—C(31)	1.462(9)	S(2)—O(23)	1.462(5)
C(31)—C(32)	1.38(1)	S(2)—O(24)	1.450(5)

<sup>a</sup> Estimated standard deviations are given in parentheses.

were located from a difference Fourier map and were positionally refined together with the corresponding non-hydrogen atoms, with one common isotropic thermal parameter ( $3.4 \text{ \AA}^2$ ). The pyridyl group hydrogen atoms were put in calculated positions, with  $\text{C—H} = 1.00 \text{ \AA}$  and were positionally refined. A unique common temperature factor was refined for these hydrogen atoms ( $4.2 \text{ \AA}^2$ ). Scattering factors and corrections for anomalous dispersion were taken from ref 37. A final difference Fourier map revealed a residual electron density between  $-1.043$  and  $+0.057 \text{ e \AA}^{-3}$ . All calculations were carried out on the Leiden University Computer (IBM 3083), using programs written or modified by E. W. Rutten-Keulemans and R.A.G.d.G. The preparation of the illustrations was done with ORTEP.<sup>38</sup>

## Results

**Description of the Structure of 1.** The molecular structure of the asymmetric dinuclear unit is depicted in Figure 1, whereas relevant bond lengths and bond angles are given in Tables 3 and 4. The cluster consists of two crystallographically independent copper(II) ions linked by the abpt ligand and a bridging sulfato anion. The  $\text{Cu(1)—Cu(2)}$  distance is  $4.415(1) \text{ \AA}$ .

The two copper(II) sites are different. The coordination sphere around Cu(1) is square pyramidal, consisting of two ligand N-donor atoms ( $\text{Cu(1)—N(2)} = 2.056(6) \text{ \AA}$ ,  $\text{Cu(1)—N(31)} = 2.048(5) \text{ \AA}$ ), the bridging sulfato oxygen ( $\text{Cu(1)—O(21)} = 1.937(4) \text{ \AA}$ ), and a monodentate coordinating sulfato anion ( $\text{Cu(1)—O(11)} = 1.891(5) \text{ \AA}$ ) in the equatorial plane and a water

(35) de Graaff, R. A. G. *Acta Crystallogr.* **1973**, *A29*, 298.

(36) Kinneging, A. J.; de Graaff, R. A. G. *J. Appl. Crystallogr.* **1984**, *17*, 364.

(37) *International Tables for X-ray Crystallography*; Kynoch Press: Birmingham, England, 1974; Vol. IV.

(38) Johnson, C. K. ORTEP. Report ORNL-3794; Oak Ridge National Laboratory: Oak Ridge, TN, 1965.

**Table 4.** Bond Angles (deg) for  $[\text{Cu}_2(\text{abpt})(\text{SO}_4)_2(\text{H}_2\text{O})_4]\cdot\text{H}_2\text{O}^a$ 

O(11)–Cu(1)–O(21)	95.8(3)	N(2)–C(3)–N(4)	108.5(6)
O(11)–Cu(1)–N(2)	155.8(2)	C(3)–N(4)–C(5)	105.4(5)
O(11)–Cu(1)–N(31)	91.4(2)	N(1)–C(5)–N(4)	110.8(5)
O(11)–Cu(1)–O(1)	104.5(2)	C(3)–N(4)–N(41)	129.5(5)
O(21)–Cu(1)–N(2)	94.8(2)	C(5)–N(4)–N(41)	125.0(5)
O(21)–Cu(1)–N(31)	172.8(3)	N(2)–C(3)–C(31)	118.7(6)
O(21)–Cu(1)–O(1)	80.0(2)	N(4)–C(3)–C(31)	132.8(6)
N(2)–Cu(1)–N(31)	78.4(2)	C(3)–C(31)–N(31)	111.6(6)
N(2)–Cu(1)–O(1)	98.8(3)	C(3)–C(31)–C(32)	125.6(6)
N(31)–Cu(1)–O(1)	98.5(2)	N(31)–C(31)–C(32)	122.7(6)
Cu(1)–O(11)–S(1)	131.4(3)	C(31)–N(31)–C(35)	119.2(6)
Cu(1)–O(21)–S(2)	121.0(3)	C(31)–C(32)–C(33)	116.6(8)
Cu(1)–N(2)–N(1)	136.6(4)	C(32)–C(33)–C(34)	120.5(7)
Cu(1)–N(2)–C(3)	114.3(5)	C(33)–C(34)–C(35)	118.5(7)
Cu(1)–N(31)–C(31)	117.0(4)	N(31)–C(35)–C(34)	122.5(7)
Cu(1)–N(31)–C(35)	123.8(5)	N(1)–C(5)–C(51)	119.1(6)
O(22)–Cu(2)–N(1)	102.7(2)	N(4)–C(5)–C(51)	130.1(6)
O(22)–Cu(2)–N(51)	173.7(2)	C(5)–C(51)–N(51)	110.7(6)
O(22)–Cu(2)–O(2)	90.0(2)	C(5)–C(51)–C(52)	126.3(6)
O(22)–Cu(2)–O(3)	92.6(2)	N(51)–C(51)–C(52)	123.0(6)
O(22)–Cu(2)–O(4)	92.3(2)	C(51)–N(51)–C(55)	118.4(6)
N(1)–Cu(2)–N(51)	78.0(2)	C(51)–C(52)–C(53)	118.2(6)
N(1)–Cu(2)–O(2)	162.7(2)	C(52)–C(53)–C(54)	118.6(6)
N(1)–Cu(2)–O(3)	87.3(2)	C(53)–C(54)–C(55)	119.6(6)
N(1)–Cu(2)–O(4)	101.1(2)	N(51)–C(55)–C(54)	122.0(7)
N(51)–Cu(2)–O(2)	90.7(2)	O(11)–S(1)–O(12)	107.8(3)
N(51)–Cu(2)–O(3)	93.7(2)	O(11)–S(1)–O(13)	107.8(3)
N(51)–Cu(2)–O(4)	81.5(2)	O(11)–S(1)–O(14)	107.6(3)
O(2)–Cu(2)–O(3)	80.4(2)	O(12)–S(1)–O(13)	111.3(3)
O(2)–Cu(2)–O(4)	90.0(2)	O(12)–S(1)–O(14)	108.9(3)
O(3)–Cu(2)–O(4)	169.2(2)	O(13)–S(1)–O(14)	113.3(3)
Cu(2)–O(22)–S(2)	130.1(3)	O(21)–S(2)–O(22)	106.7(3)
Cu(2)–N(1)–N(2)	138.3(4)	O(21)–S(2)–O(23)	108.8(3)
Cu(2)–N(1)–C(5)	113.4(4)	O(21)–S(2)–O(24)	110.8(3)
Cu(2)–N(51)–C(51)	116.6(4)	O(22)–S(2)–O(23)	108.1(3)
Cu(2)–N(51)–C(55)	125.0(5)	O(22)–S(2)–O(24)	108.4(3)
N(2)–N(1)–C(5)	106.1(5)	O(23)–S(2)–O(24)	108.4(3)
N(1)–N(2)–C(3)	109.1(5)		

<sup>a</sup> Estimated standard deviations are given in parentheses.

molecule in the apical position (Cu(1)–O(1) = 2.2475(5) Å). Cu(2) is in a tetragonally distorted octahedron formed by two abpt N-donor atoms (Cu(2)–N(1) = 2.038(5) Å, Cu(2)–N(51) = 2.061(6) Å), an oxygen atom of the  $\mu$ -sulfato anion (Cu(2)–O(22) = 1.908(5) Å), and a water molecule in the equatorial plane (Cu(2)–O(2) = 2.001(5) Å). Two additional water molecules coordinate axially (Cu(2)–O(3) = 2.411(7) Å, Cu(2)–O(4) = 2.430(5) Å).

The abpt ligand acts as a planar doubly didentate chelating ligand, with N(1) and N(2) as bridging atoms between the copper(II) ions, which is a well-known coordination mode for transition-metal(II) ions.<sup>5–13,28</sup> The pyridyl groups are slightly twisted with respect to the 1,2,4-triazole ring. The dihedral angle between these rings and the triazole is 9.6(3)° for both pyridyl groups, significantly larger than observed in the doubly  $N^1,N^2$  bridged 3,5-bis(pyridin-2-yl)-1,2,4-triazolato (abbreviated as bpt)<sup>8</sup> and 3-(pyridin-2-yl)-1,2,4-triazolato (abbreviated as pt)<sup>11,12</sup> dinuclear copper(II) compounds. One would expect that in  $[\text{Cu}_2(\text{abpt})(\text{SO}_4)_2(\text{H}_2\text{O})_4]\cdot\text{H}_2\text{O}$  the ligand has a more favorable geometrical conformation, which is possible since there is no steric hindrance from other groups (*i.e.*, another abpt ligand) on the other side of the plane. As a consequence, the Cu–N(pyridine) and Cu–N(triazole) distances are similar, whereas in the related bpt<sup>8</sup> and pt<sup>11,12</sup> dimers the Cu–N(pyridine) distances are significantly longer than the Cu–N(triazole) distances. On the other hand, the N(pyridine)–Cu–N(triazole) bite angles are comparable for all compounds.<sup>8,11,12</sup> The  $N^1,N^2$  1,2,4-triazole bridging mode is a relatively symmetric one, which is also reflected in the Cu(1)–N(2)–N(1) and Cu(2)–N(1)–N(2) angles, which are 136.6(4) and 138.3(4)°, respectively.

**Table 5.** Interatomic Distances (Å) and Angles (deg) for the Hydrogen-Bonding Interactions in  $[\text{Cu}_2(\text{abpt})(\text{SO}_4)_2(\text{H}_2\text{O})_4]\cdot\text{H}_2\text{O}^a$ 

D	H <sup>b</sup>	A	D–H	H···A	D···A	D–H···A
O(12)		O(1)			2.816(8)	
O(12)		O(2) <sup>1</sup>			2.657(6)	
O(13)		O(4) <sup>1</sup>			2.693(7)	
O(14)		O(3) <sup>2</sup>			2.677(8)	
O(21)		O(1)			2.699(6)	
O(22)		O(2)			2.764(7)	
O(1) <sup>3</sup>	H(11) <sup>3</sup>	O(23)	0.9322	1.817(7)	2.723(7)	163.5(2)
O(23)		O(3)			2.870(9)	
O(4) <sup>1</sup>	H(41) <sup>1</sup>	O(23)	0.7750	2.241(7)	2.861(7)	137.6(2)
O(2)		O(3)			2.865(8)	
O(2)	H(21)	O(5) <sup>4</sup>	0.7543	2.081(9)	2.761(9)	150.2(2)
O(5) <sup>5</sup>	H(52) <sup>5</sup>	O(4)	0.8728	1.922(9)	2.775(9)	165.5(3)

<sup>a</sup> Estimated standard deviations are given in parentheses. Atoms marked with a number are generated by symmetry operations: 1 = 1 – x, –0.5 + y, –z; 2 = –x, –0.5 + y, –z; 3 = x, y, 1 + z; 4 = –x, 0.5 + y, 1 – z; 5 = –x, 0.5 + y, –z. <sup>b</sup> The positions of not all hydrogen atoms could be determined.

The bridging mode is therefore comparable to the one found in the bpt<sup>8</sup> and 4-amino-3,5-bis(aminomethyl)-1,2,4-triazole (abbreviated as aamt)<sup>9,10</sup> copper(II) compounds, although in these compounds the angles are almost identical (between 132.9(8) and 135.2(2)°). This is in contrast with the asymmetric bridging mode observed in the pt compounds,<sup>11,12</sup> where the Cu(1)–N(2)–N(1) angles range from 123.9(3) to 126.0(2)° and the Cu(2)–N(1)–N(2) angles from 138.7(2) to 140.0(2)°. These structural differences result in a Cu(1)–Cu(2) distance of 4.415–(1) Å for the present compound, which is 0.3–0.4 Å longer than for all other doubly  $N^1,N^2$  1,2,4-triazole bridged copper(II) dimers.<sup>8–12</sup>

Furthermore, a bridging sulfate links the copper(II) ions in the equatorial plane. Although  $\mu$ -sulfato-*O,O'* groups have been reported in the literature, these are relatively rare.<sup>39,40</sup> The bond distances found in this compound for Cu(1)–O(21) and Cu(2)–O(22) are 1.937(4) and 1.908(5) Å, respectively. These are among the shortest copper(II)–O( $\mu$ -sulfato)<sup>39,40</sup> and copper(II)–O( $\mu_3$ -sulfato)<sup>41–43</sup> distances reported up to now. This short bond arises from the fact that both coordinating oxygen atoms of the sulfato group are in the equatorial coordination sphere of copper(II), whereas in most other cases the sulfate bridges in an axial position.

The structure is stabilized by an extensive network of hydrogen bonds (see Table 5). All noncoordinating oxygen atoms of the sulfates as well as all coordinating and noncoordinating water molecules are involved in hydrogen bonding. The asymmetric dinuclear cluster is stabilized in particular by the hydrogen bonds which are formed between the oxygens of the monodentate to Cu(2) coordinating sulfate and the water molecules which are coordinated to Cu(1) of two dinuclear units which are generated by symmetry operations 1 – x, –0.5y, –z and –x, –0.5y, –z.

**Electronic and IR Spectra.** The inequality of the two copper(II) chromophores in **1** is reflected in the UV/vis spectrum, which shows a very broad band centered around  $12.3 \times 10^3 \text{ cm}^{-1}$ . This position is in agreement with the presence of tetragonally based  $\text{CuN}_2\text{O}_3$  and  $\text{CuN}_2\text{O}_4$  chromophores.<sup>44</sup>

(39) Endres, H.; Nöthe, P.; Rossato, E.; Hatfield, W. E. *Inorg. Chem.* **1984**, *23*, 3467.

(40) Knuutila, P. *Inorg. Chim. Acta* **1982**, *58*, 201.

(41) Thompson, L. K.; Hanson, A. W.; Ramaswamy, B. S. *Inorg. Chem.* **1984**, *23*, 2459.

(42) Beckett, R.; Hoskins, B. F. *J. Chem. Soc., Dalton Trans.* **1972**, 291.

(43) Beckett, R.; Colton, R.; Hoskins, B. F.; Martin, R. L.; Vince, D. G. *Aust. J. Chem.* **1969**, *22*, 2527.

(44) Hathaway, B. J.; Billing, D. E. *Coord. Chem. Rev.* **1970**, *5*, 143.

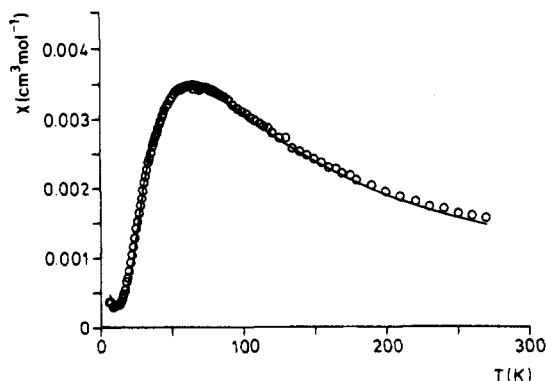


**Figure 2.**  $\chi$  vs  $T$  curve for  $[\text{Cu}_2(\text{abpt})(\text{SO}_4)_2(\text{H}_2\text{O})_4]\cdot\text{H}_2\text{O}$ . The solid line represents the calculated curve ( $J = -34.5 \text{ cm}^{-1}$ ,  $g = 2.15$ ,  $p = 0.66\%$ ).

The  $T_d$  symmetry of the sulfate is reduced to  $C_{3v}$  due to monodentate coordination and to  $C_{2v}$  upon didentate bridging coordination to copper(II). The absorptions observed in the infrared spectrum are in agreement with the presence of sulfates of both symmetries: 1195 ( $\nu_3$ ), 1125 ( $\nu_3$ ), 1040 ( $\nu_3$ ), 987 ( $\nu_1$ ), 648 ( $\nu_4$ ), 605 ( $\nu_4$ ), 438 ( $\nu_2$ )  $\text{cm}^{-1}$ .<sup>45</sup>

**Magnetic Properties.** The magnetic susceptibility was recorded in the 295–6 K region. For **1** the behavior of a copper(II) dinuclear compound was found with a maximum in the  $\chi$  vs  $T$  curve at ca. 60 K (see Figure 2). The magnetic data for compound **1** were fitted to the modified Bleaney–Bowers expression for the molar magnetic susceptibility for  $S = 1/2$  dimers<sup>46</sup>

$$\chi_m = \frac{2N\beta^2 g^2}{kT} [3 + \exp(-2J/kT)]^{-1} (1 - p) + \chi_p p \quad (1)$$

in which  $2J$  is the singlet–triplet energy gap defined by the phenomenological spin Hamiltonian with quantum spin operators  $\hat{S}_{\text{Cu}(1)}$  and  $\hat{S}_{\text{Cu}(2)}$

$$\hat{H} = -2J(\hat{S}_{\text{Cu}(1)} \cdot \hat{S}_{\text{Cu}(2)}) \quad (2)$$

In eq 1,  $N$ ,  $g$ ,  $\beta$ ,  $k$ , and  $T$  have their usual meanings. The parameter  $p$  denotes the percentage of paramagnetic impurity present in the sample. A good fit has been obtained for the parameters  $J = -34.5 \text{ cm}^{-1}$ ,  $g = 2.15$ , and  $p = 0.66\%$ . Figure 2 depicts the calculated and observed curves.

To explain the magnitude of the isotropic magnetic exchange interaction, we first focus on how the superexchange is propagated. In this compound, the unpaired electron of the copper(II) ion is in a magnetic orbital of  $d(x^2 - y^2)$  symmetry, which is situated in the plane of the equatorial coordination sphere around the copper(II) ions; it is partially delocalized on the equatorial ligands. The two  $d(x^2 - y^2)$  magnetic orbitals overlap through the  $N^1, N^2$  1,2,4-triazole bridge and the  $\mu$ -sulfato anion. Therefore, the observed magnetic interaction must be resolved in contributions arising from each Cu–ligand–Cu linkage. It has been reported that the  $\mu$ -sulfato ligand is moderately effective in transmitting the superexchange.<sup>39</sup> This has been deduced from the magnetic data for bis[( $\mu$ -sulfato)-aqua(oxamide dioxime)copper(II)],  $[\text{Cu}(\text{C}_2\text{H}_6\text{N}_4\text{O}_2)(\text{H}_2\text{O})(\text{SO}_4)]_2$ . The magnetic interaction between the copper(II) ions separated by 5.087(2) Å and linked by two sulfato anions (Cu–O = 2.375-(3) and 1.946(3) Å) was characterized by a singlet–triplet

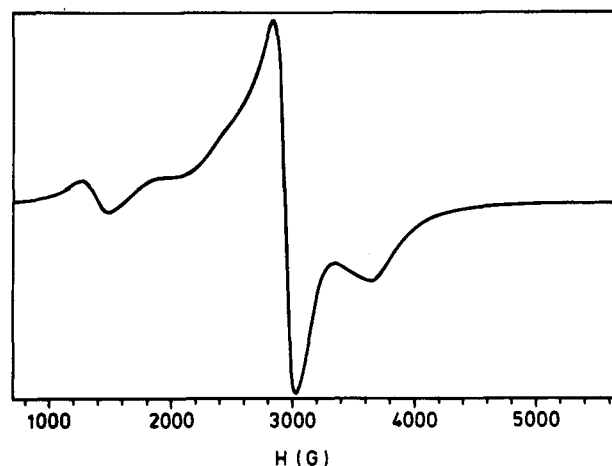


**Figure 3.** X-Band (9.04 GHz) powder EPR spectrum of  $[\text{Cu}_2(\text{abpt})(\text{SO}_4)_2(\text{H}_2\text{O})_4]\cdot\text{H}_2\text{O}$  recorded at 50 K.

splitting  $2J = -2.55 \text{ cm}^{-1}$ .<sup>39</sup> It should be noted that, in this compound, the sulfate does not link the copper(II) ions in the equatorial plane; moreover, the Cu(II)–Cu(II) separation is much shorter in  $[\text{Cu}_2(\text{abpt})(\text{SO}_4)_2(\text{H}_2\text{O})_4]\cdot\text{H}_2\text{O}$ . In all other reported  $\mu$ -sulfato compounds, the anion is part of a bridging network consisting of different ligands,<sup>40,41</sup> which makes it very difficult to deduce the contribution arising from the superexchange pathway *via* the sulfate. However, it may be expected that, in compound **1**, the most important pathway for magnetic exchange is propagated *via* the bridging 1,2,4-triazole. Clearly, the interaction *via* a double bridge should be larger than that *via* a single 1,2,4-triazole bridge of an identical geometry. We recall that when two copper(II) ions are bridged by extended ligands, such as the  $\mu$ - $N^1, N^2$  triazole, the ferromagnetic contribution to the exchange is very small and only the antiferromagnetic contribution is significant. This antiferromagnetic contribution is proportional to the square of the overlap integral of the magnetic orbitals.<sup>2,4</sup> Thus, two identical bridging ligands are expected to produce an exchange constant  $J_{\text{AF}}$ , which is 4 times larger than the exchange constant caused by one ligand alone.<sup>47,48</sup> The geometry of the bridging 1,2,4-triazole network resembles mostly those of the symmetric doubly  $N^1, N^2$  1,2,4-triazole bridged dinuclear copper(II) compounds.<sup>8–10</sup> For these bpt<sup>8</sup> and aamt<sup>9,10</sup> compounds, the values for the exchange parameter  $J$  are in the range  $-97$  to  $-118 \text{ cm}^{-1}$ . It may then be assumed that the maximal  $J$  value for two copper(II) ions linked by a single  $N^1, N^2$  1,2,4-triazole bridge is about  $-30 \text{ cm}^{-1}$ . This value has indeed been observed experimentally for  $\{[\text{Cu}_3(\text{tcz})_2(\text{dien})(\text{H}_2\text{O})_2](\text{H}_2\text{O})_3\}_\infty$  (tcz = 3,5-bis(carboxylato)-1,2,4-triazolate; dien = 1,4,7-triazaheptane).<sup>13</sup> In fact, the present isotropic exchange constant of  $-34.5 \text{ cm}^{-1}$  is close to this value. Nevertheless, it may not be correct to compare these values, since it cannot be excluded that there is some contribution from the exchange pathway *via* the bridging sulfate. Furthermore, there are some other structural differences between the present abpt compound and the bpt and aamt compounds: the geometry of the bridging triazole ligands is not exactly identical, the Cu–Cu distance is significantly longer in the abpt compound, and there are differences in coordination geometry of the copper(II) ions.

**Powder and Single-Crystal EPR Spectra.** The X-band polycrystalline powder EPR spectra of **1** were recorded at temperatures between 20 and 298 K. The spectrum recorded at 50 K is depicted in Figure 3. The spectra are characteristic

(45) Nakamoto, K. *Infrared and Raman Spectra of Inorganic and Coordination Compounds*, 3rd ed.; Wiley: New York, 1978.

(46) Bleaney, B.; Bowers, K. D. *Proc. R. Soc. London, Ser. A* **1952**, *214*, 451.

(47) Mayer, I.; Angelov, S. *J. Phys. C: Solid State Phys.* **1983**, *16*, L857.

(48) Atanasov, M.; Angelov, S.; Mayer, I. *J. Mol. Struct.* **1989**, *187*, 23.

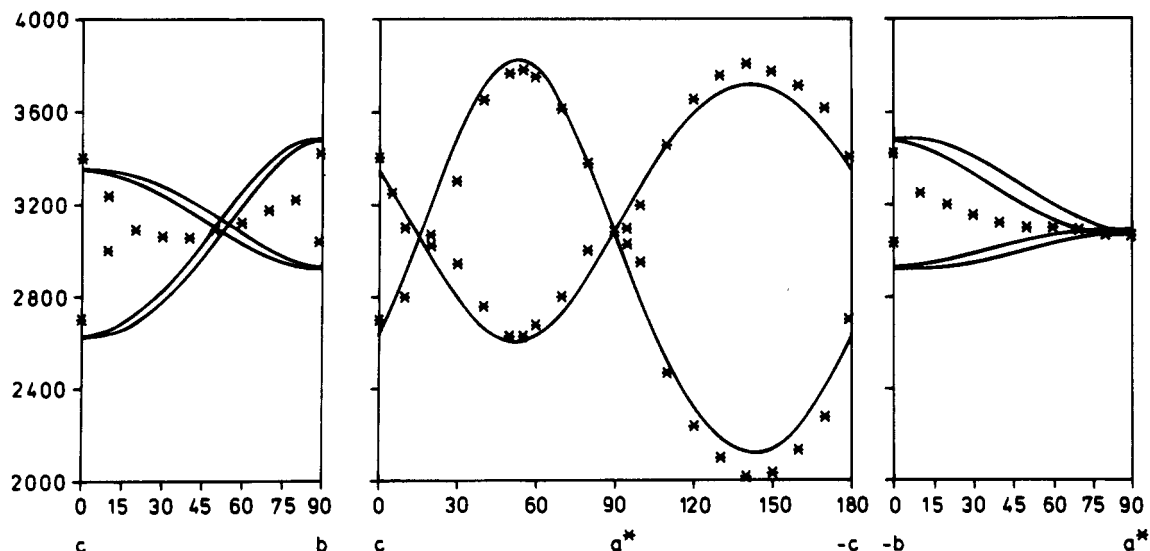


**Figure 4.** Angular dependence of the transition fields (in tesla) for  $[\text{Cu}_2(\text{abpt})(\text{SO}_4)_2(\text{H}_2\text{O})_4]\cdot\text{H}_2\text{O}$  (X-band frequency, room temperature). The crystal axes are defined in the text.

of a triplet spin state with an anisotropic zero-field-splitting tensor.<sup>26</sup> The normal feature for a copper(II) dimer, the half-field signal at  $g = 4.30$ , is observed. The Q-band EPR spectrum recorded at 22 K shows signals at effective  $g$  values of 2.39, 2.04, and 1.88.

Single-crystal EPR spectra at room temperature were recorded at X-band frequency by rotating the crystal with respect to the static magnetic field around three orthogonal axes (laboratory frame)  $a$ ,  $b$ ,  $c$ . The  $a$  axis is perpendicular to the (100) crystal face, the  $b$  axis is perpendicular to (010), and the  $c$  axis is defined by the intersection of the (100) and (010) crystal faces. The EPR spectra were recorded by rotating the static magnetic field in the (100), (001), and (010) planes, *i.e.* in the planes  $cb$ ,  $a^*c$ , and  $a^*b$ , respectively, in the laboratory frame. Taking into account that the  $b$  axis is the unique axis in the monoclinic cell, which contains two asymmetric dinuclear copper(II) species, signals arising from two nonequivalent Cu(II) sites are expected during rotation in the (001) and (100) planes, whereas in the (010) plane only one signal corresponding to one kind of copper(II) site is expected.<sup>26</sup> In the present case, indeed a typical spectrum, *i.e.*, two lines split by the zero-field parameter  $D$ , are observed in the (010) plane. However, only one signal is observed by rotating in the (100) and (001) planes (instead of the expected four lines). This indicates that the dinuclear species are not perfectly isolated and intermolecular magnetic exchange interactions are operative, allowing the signals to merge into one. For the same reason the lines are rather broad. On the other hand, the relatively small value for the zero-field-splitting parameter may not allow the observation of separate lines in the EPR spectra, leading to the broad band observed. Due to the broad lines, a detailed analysis of the spectra is difficult. The EPR data are interpreted from the spin Hamiltonian associated with the molecular triplet spin state  $S = 1$ :

$$\hat{H} = \beta\mathbf{H}\cdot\mathbf{g}\mathbf{S} + \mathbf{S}\cdot\mathbf{D}\cdot\mathbf{S} \quad (3)$$

The angular dependence of the transition fields in the three rotations and the best-fit curves, obtained with a procedure described previously,<sup>49</sup> are shown in Figure 4. The best-fit spin Hamiltonian parameters, together with experimental errors, as well as the directions of the  $\mathbf{g}$  and  $\mathbf{D}$  tensors, which were obtained by the Schonland procedure,<sup>50</sup> are given in Table 6.

**Table 6.** Principal Values and Directions of  $\mathbf{g}$  and  $\mathbf{D}$  Tensors for  $[\text{Cu}_2(\text{abpt})(\text{SO}_4)_2(\text{H}_2\text{O})_4]\cdot\text{H}_2\text{O}^{a,b}$

$g_{xx} = 2.09(3)$	$g_{yy} = 2.10(3)$	$g_{zz} = 2.32(2)$
-0.5(8)	-0.6(6)	-0.58(5)
-0.8(8)	0.6(9)	0.0(1)
-0.4(5)	-0.5(4)	0.81(4)
$D_{x'x'} = 0.018(2)^c$	$D_{y'y'} = 0.04(3)^c$	$D_{z'z'} = -0.058(3)^c$
0.11(9)	-0.79(2)	0.61(1)
-0.99(2)	-0.1(1)	0.01(3)
0.08(8)	-0.60(2)	-0.79(1)

<sup>a</sup> The directions with respect to the crystal faces are given in the text. <sup>b</sup> Estimated standard deviations are given in parentheses. <sup>c</sup> The principal values for the  $\mathbf{D}$  tensor are given in  $\text{cm}^{-1}$ .

The  $\mathbf{g}$  directions in the  $xy$  plane are affected by a large experimental error, due to the very small anisotropy of  $\mathbf{g}$  in this plane. The  $g_{zz}$  and  $D_{z'z'}$  directions are almost parallel; the angle between these vectors is only  $2^\circ$ . These vectors make an angle of about  $12^\circ$  with the vector normal to the Cu(1)–Cu(2) coordination plane.

From these data, the powder spectrum was interpreted by assuming that  $\mathbf{g}$  and  $\mathbf{D}$  were coincident, which is not rigorously exact. Upon substitution of the parameters obtained (*i.e.*,  $g_x = 2.09$ ,  $g_y = 2.10$ ,  $g_z = 2.32$ ,  $|\mathbf{D}| = 0.0867 \text{ cm}^{-1}$ ,  $|\mathbf{E}| = 0.0113 \text{ cm}^{-1}$ ,  $\mathbf{E}/\mathbf{D} = 0.13$ ) into the formulas reported for the transition fields along the principal axes,<sup>51</sup> the X-band powder EPR spectra are reproduced fairly.

The zero-field-splitting tensor  $\mathbf{D}$  shows evidence of substantial exchange contributions. In fact, the largest component is not found to be parallel to the Cu(1)–Cu(2) direction, as would be expected for dominant dipolar effects,<sup>52</sup> but to the  $g_{zz}$  direction. The same features have also been found for  $[\text{Cu}(\text{bpt})(\text{CF}_3\text{SO}_3)(\text{H}_2\text{O})_2]$  (bpt = 3,5-bis(pyridin-2-yl)-1,2,4-triazolato)<sup>7</sup> and  $[\text{Cu}(\text{ppt})(\text{H}_2\text{O})_4(\text{NO}_3)_4(\text{H}_2\text{O})_{12}]$  (ppt = 3-(pyridin-2-yl)-5-(pyrazin-2-yl)-1,2,4-triazolato)<sup>5</sup> and for a series of bis( $\mu$ -hydroxo)-bridged copper(II) complexes.<sup>49,53–55</sup>

(50) Schonland, D. S. *Proc. Phys. Soc. London* **1959**, *73*, 788.

(51) Wasson, J. R.; Shyr, C.; Trapp, C. *Inorg. Chem.* **1968**, *7*, 469.

(52) Gatteschi, D.; Bencini, A. In *Magneto-structural correlations in exchange coupled systems*; Gatteschi, D., Kahn, O., Willett, R. D., Eds.; NATO Advanced Study Institute Series; D. Reidel: Dordrecht, Holland, 1984; Vol. C140.

(53) Banci, L.; Bencini, A.; Gatteschi, D. *J. Am. Chem. Soc.* **1983**, *105*, 761.

(54) Bencini, A.; Gatteschi, D.; Zanchini, C. *Inorg. Chem.* **1985**, *24*, 700.

(49) Banci, L.; Bencini, A.; Gatteschi, D.; Zanchini, C. *J. Magn. Reson.* **1982**, *48*, 9.

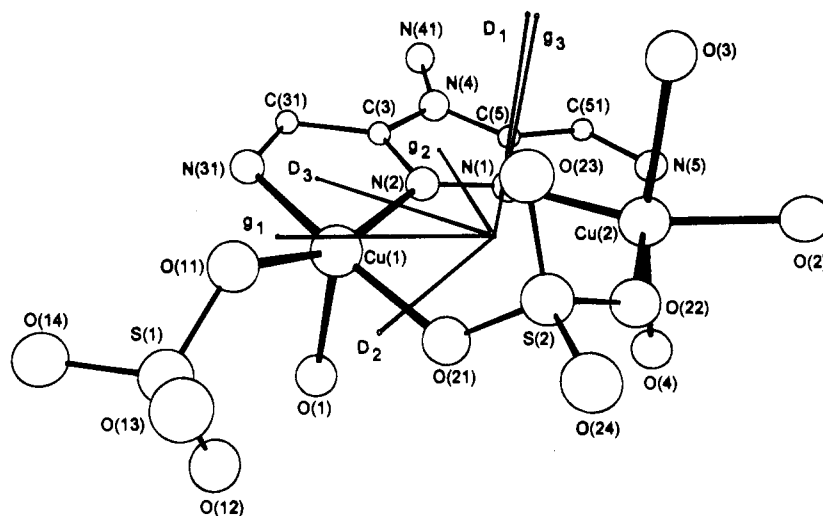


**Figure 5.** ORTEP<sup>38</sup> projection of  $[\text{Cu}_2(\text{abpt})(\text{SO}_4)_2(\text{H}_2\text{O})_4]\cdot\text{H}_2\text{O}$  showing the principal directions of the  $g$  and  $D$  tensors. The pyridyl groups of the abpt ligand have been omitted for clarity.

The zero-field-splitting parameter  $D$  for a Cu(II)–Cu(II) couple is determined by two main contributions: a direct magnetic interaction between the unpaired electron spins (often referred to as the magnetic dipolar exchange  $D^{\text{dip}}$ ) and an anisotropic exchange interaction ( $D^{\text{ex}}$ ).<sup>53,56</sup> The dipolar contribution is usually calculated in the approximation of magnetic dipoles centered on the metal ions.<sup>57</sup> With this assumption  $D^{\text{dip}}$  is easily calculated in the  $g$  reference frame. Upon diagonalization, the principal values and directions of the calculated dipolar tensor are obtained:  $D_{xx}^{\text{dip}} = -4.52 \times 10^{-2} \text{ cm}^{-1}$ ,  $D_{yy}^{\text{dip}} = -9.94 \times 10^{-4} \text{ cm}^{-1}$ ,  $D_{zz}^{\text{dip}} = 0 \text{ cm}^{-1}$ ,  $D_{xy}^{\text{dip}} = 2.04 \times 10^{-2} \text{ cm}^{-1}$ ,  $D_{yz}^{\text{dip}} = 0 \text{ cm}^{-1}$ ,  $D_{zx}^{\text{dip}} = 0.0278 \text{ cm}^{-1}$ . The directions are defined as follows:  $x$  is parallel to the Cu(1)–Cu(2) direction,  $y$  is perpendicular to this direction, and  $z$  makes an angle of  $2^\circ$  with the normal vector of the Cu(1)Cu(2) coordination plane.

The exchange contribution to the axial zero-field splitting is calculated by subtraction of the dipolar contribution from the experimentally determined  $D$  tensor:

$$D^{\text{ex}} = D - D^{\text{dip}} \quad (4)$$

According to the two possible choices of sign for the experimental  $D$  tensor, two  $D^{\text{ex}}$  tensors are obtained, which, through a standard analysis,<sup>26,53,58–60</sup> yield a ferromagnetic coupling between the  $d(x^2 - y^2)$  ground magnetic orbital of an ion and the  $d(xy)$  excited magnetic orbital of the other ion. The use of tensor  $D_1^{\text{ex}}$  yields  $J_{x^2-y^2,xy} = +38.3 \text{ cm}^{-1}$ , whereas  $D_2^{\text{ex}}$  yields  $J_{x^2-y^2,xy} = +15.4 \text{ cm}^{-1}$ . For this compound, in either case a sizable ferromagnetic interaction has been calculated for the anisotropic exchange integral involving the ground  $d(x^2 - y^2)$  orbital of one ion and the excited  $d(xy)$  orbital on the other ion.

This value for  $J_{x^2-y^2,xy}$  cannot be compared directly to that for  $[\text{Cu}(\text{bpt})(\text{CF}_3\text{SO}_3)(\text{H}_2\text{O})_2]_2$ ,<sup>7</sup> since in that case its precise value has not been reported. However, from the similarity in magnitudes and principal directions of the  $g$  and  $D$  tensors, as well as a comparable dipolar contribution to the axial zero-

field splitting, it may be concluded that the exchange contributions are of the same magnitude. This implies that the anisotropic exchange propagation capabilities of bridging networks consisting respectively of one and two 1,2,4-triazole ligands are comparable.

### Conclusion

The compound  $[\text{Cu}_2(\text{abpt})(\text{SO}_4)_2(\text{H}_2\text{O})_4]\cdot\text{H}_2\text{O}$  represents the first example of a dinuclear copper(II) compound containing a single  $N^1, N^2$  1,2,4-triazole bridge. It is remarkable that this compound is highly asymmetric. The present compound shows that anions other than monoatomic ones, such as the well-known hydroxo,<sup>61</sup> fluoro,<sup>62</sup> and chloro<sup>63–66</sup> bridges, can, together with  $\mu$ - $N^1, N^2$  1,2,4-triazoles, constitute the bridging network. The  $\mu$ -sulfato anion links the copper(II) ions in the equatorial plane with very short Cu–O distances.

It is known that in a nonsymmetrical dinuclear compound, the antisymmetric interaction is expected to contribute significantly to the axial zero-field splitting. The effect of this antisymmetric interaction is expected to vanish not only when the complex is centrosymmetric but also when its symmetry is  $C_{nv}$  (with  $n$  larger than or equal to 2) and the  $n$ -fold axis joining the interacting centers is 2-fold or higher. It has, therefore, been stated that, for most of the reported compounds, the antisymmetric interaction is zero.<sup>67</sup> Indeed, this interaction has not yet been observed experimentally.<sup>4,67</sup> The present dinuclear compound appears to have the right symmetry requirements to allow the antisymmetric interaction to be detected. However, in spite of the fact that, in the present compound, the copper(II) ions are not related by an inversion center nor is a  $C_{nv}$  axis present, the contribution of the antisymmetric interaction has been estimated to be quite weak. This small interaction originates from the fact that, in spite of the different coordination environments around both copper(II) ions, the local  $g$  tensors are rather similar. Furthermore, generally, the antisymmetric interaction is expected to be very small; the quality of our measurements does not allow its determination, in case this

(55) Gatteschi, D. *J. Mol. Catal.* **1984**, *23*, 145.

(56) Owen, J.; Harris, E. A. *Electron Paramagnetic Resonance*; Geshwind, S., Ed.; Plenum Press: New York, 1972; pp 427–492.

(57) Abragam, A.; Bleaney, B. *Electron Paramagnetic Resonance of Transition Ions*; Clarendon Press: London, 1970; pp 492–495.

(58) Moriya, T. *Phys. Rev.* **1960**, *120*, 91.

(59) Moriya, T. In *Magnetism*; Rado, G. T., Suhl, H., Eds.; Academic Press: New York, 1963; Vol. 1, p 85.

(60) Banci, L.; Bencini, A.; Gatteschi, D. *Inorg. Chem.* **1984**, *23*, 2138.

(61) Vreudgenhil, W. Ph.D. Thesis, Leiden University, 1987.

(62) Keij, F. S. Ph.D. Thesis, Leiden University, 1990.

(63) van Koningsbruggen, P. J.; van Hal, J. W.; de Graaff, R. A. G.; Haasnoot, J. G.; Reedijk, J. *J. Chem. Soc., Dalton Trans.* **1993**, 2163.

(64) Jarvis, J. A. *J. Acta Crystallogr.* **1962**, *15*, 964.

(65) Inoue, M.; Emori, S.; Kubo, M. *Inorg. Chem.* **1968**, *7*, 1427.

(66) Inoue, M.; Kubo, M. *Coord. Chem. Rev.* **1976**, *21*, 1.

(67) Kahn, O.; Pei, Y.; Journaux, Y. In *Inorganic Materials*; Bruce, D. W., O'Hare, D., Eds.; Wiley: New York, 1992; p 59.

interaction would be present. Thus, the present analysis of the *D* tensor in terms of dipolar and exchange contributions to the zero-field splitting is justified.

The data available from single-crystal EPR studies allow a comparison among the anisotropic exchange propagation capabilities of various ligand systems. A borderline case is represented by the dinuclear copper(II) compounds containing a double monoatomic bridge, such as hydroxo,<sup>49,53–55</sup> alkoxy,<sup>68</sup> chloro,<sup>69</sup> and  $\mu$ -1,1-azido,<sup>70</sup> where the exchange contribution to the zero-field splitting is very small. On the other hand, polyatomic ligands, such as oxalato<sup>71</sup> and oxamido,<sup>72</sup> have been found to be very effective in transmitting the isotropic exchange but not effective at all in transmitting the anisotropic exchange. The present study confirms that the 1,2,4-triazole ligand can be regarded as an intermediate case; *i.e.*, the ligand is moderately effective in transmitting the isotropic exchange, as well as the anisotropic exchange.<sup>5,7</sup> The single-crystal EPR data reported for a bis(pyrazolato) and monochloro bridged dinuclear copper(II) compound<sup>73</sup> are to a certain extent comparable to those for the  $N^1, N^2$  1,2,4-triazole bridged copper(II) compounds; *i.e.*, similar magnitudes and principal directions of the *g* and *D* tensors have been found. However, the analysis of these data resulted in peculiar values for the anisotropic exchange contribution, which possibly might be due to the presence of the bridging chloride in axial position.

(68) Bencini, A.; Gatteschi, D.; Zanchini, C.; Haase, W. *Inorg. Chem.* **1985**, *24*, 3485 (and references therein).

(69) Bencini, A.; Gatteschi, D.; Zanchini, C. *Inorg. Chem.* **1985**, *24*, 704.

(70) Boillot, M.-L.; Journaux, Y.; Bencini, A.; Gatteschi, D.; Kahn, O. *Inorg. Chem.* **1985**, *24*, 263.

(71) Bencini, A.; Fabretti, A. C.; Zanchini, C.; Zannini, P. *Inorg. Chem.* **1987**, *26*, 1445.

(72) Bencini, A.; Di Vaira, M.; Fabretti, A. C.; Gatteschi, D.; Zanchini, C. *Inorg. Chem.* **1984**, *23*, 1620.

(73) Ajò, D.; Bencini, A.; Mani, F. *Inorg. Chem.* **1988**, *27*, 2437.

From the present study it can be concluded that the anisotropic exchange *via* a single 1,2,4-triazole bridge is comparable to that *via* a double 1,2,4-triazole bridge. On the other hand, our results show the isotropic exchange *via* a single  $N^1, N^2$  1,2,4-triazole bridge to be about 4 times smaller than that *via* a double  $N^1, N^2$  1,2,4-triazole bridge of a similar geometry. Since these exchange effects arise from different mechanisms of exchange, the observations cannot be correlated. However, apparently, the anisotropic exchange seems to be less sensitive to the presence of a single or a double ligand bridge. Unfortunately, no other studies involving similar copper(II) compounds with a single and a double ligand bridge have been reported. This implies that further studies are required to shed more light on the phenomenon of anisotropic exchange interaction.

**Acknowledgment.** The authors thank the Werkgroep Fundamenteel Materialen Onderzoek (WFMO) for financial support. Mr. S. Gorter is acknowledged for the X-ray data collection; R. Sessoli and A. Caneschi helped us to determine the Miller indices of the crystal faces. This work was supported in part (P.J.v.K.) by the Netherlands Foundation of Chemical Research (SON) with financial aid from the Netherlands Foundation for Scientific Research (NWO). Financial support from the European Union, allowing regular exchange of preliminary results with several European colleagues, under Contract ERBCHRX-CT920080 is gratefully acknowledged.

**Supporting Information Available:** Tables giving intensity data collection parameters, anisotropic thermal parameters, positional and thermal parameters for hydrogen atoms, and selected least-squares planes (7 pages). Ordering information is given on any current masthead page.

IC9500523